

Indexed by

Scopus®DOAJ
DIRECTORY OF
OPEN ACCESS
JOURNALSCrossrefROAD
DIRECTORY OF OPEN ACCESS
RESEARCH RESOURCESKoBSONSCINDEKS
Srpski citatni indeksGoogle
Scholar

NUMERICAL ANALYSIS OF LIGHTWEIGHT CONCRETE WALL PANELS HAVING A VARIATION OF DIMENSIONS AND OPENINGS THAT WERE SUBJECTED TO STATIC LATERAL LOADS

Siti Aisyah Nurjannah

Civil Engineering
Department, Faculty of
Engineering, Universitas
Sriwijaya, Indonesia

Saloma

Civil Engineering
Department, Faculty of
Engineering, Universitas
Sriwijaya, Indonesia

Hanafia

Civil Engineering
Department, Faculty of
Engineering, Universitas
Sriwijaya, Indonesia

Nadia Darin Putr

Civil Engineering
Department, Faculty of
Engineering, Universitas
Sriwijaya, Indonesia

Fadel Satria Albimanzur

Civil Engineering
Department, Faculty of
Engineering, Universitas
Sriwijaya, Indonesia

Key words: ductility, lateral load, lightweight concrete, wall panel, wire mesh
doi:10.5937/jaes0-31011

Cite article:

Aisyah Nurjannah S., Saloma., Hanafia., Darin Putr N., Satria Albimanzur F. (2022) NUMERICAL ANALYSIS OF LIGHTWEIGHT CONCRETE WALL PANELS HAVING A VARIATION OF DIMENSIONS AND OPENINGS THAT WERE SUBJECTED TO STATIC LATERAL LOADS, *Journal of Applied Engineering Science*, 20(1), 109 - 122, DOI:10.5937/ jaes0-31011

Online access of full paper is available at: www.engineeringscience.rs/browse-issues

NUMERICAL ANALYSIS OF LIGHTWEIGHT CONCRETE WALL PANELS HAVING A VARIATION OF DIMENSIONS AND OPENINGS THAT WERE SUBJECTED TO STATIC LATERAL LOADS

Siti Aisyah Nurjannah*, Saloma, Hanafiah, Nadia Darin Putri, Fadel Satria Albimanzura
Civil Engineering Department, Faculty of Engineering, Universitas Sriwijaya, Indonesia

Wall panels are non-structural parts of buildings that are considered dead loads. The mass of wall panels must be reduced to minimize earthquake risk and enhance structural resistance to lighter dead loads. This study used wall panel models that consisted of lightweight foamed concrete materials containing expanded polystyrene. The wall panels used in this study also had a variety of dimensions and reinforcements. The effect of openings on wall panel model performance was also investigated. This study aimed to analyze the performance of lightweight concrete wall panel models under static lateral loads applied until the ultimate condition. It was found that the load-deformation relation performs varying values of stiffness, strength, and ductility depended on the wall panel dimensions, reinforcements, and openings. A wall panel model with a height of 1000 mm that had length of 1500 mm and thickness of 60 mm with wire mesh and without openings achieved the highest ultimate stiffness and strength. The highest ductility was achieved by a wall panel model with openings, without wire mesh, with height, length, and thickness of 1500 mm, 1500 mm, and 40 mm, respectively. Diagrams of the deformations in this paper reflect the compressed and tensioned areas. The lefthand parts of all wall panel models without wire mesh were tensioned and had concentrations of deformation in those areas. The existence of openings also caused increased deformation due to less stiffness in the wall panel models.

Key words: ductility, lateral load, lightweight concrete, wall panel, wire mesh

INTRODUCTION

Wall panels are commonly used for partitioning spaces in buildings [1]. The materials used for wall panels are made up of non-structural concrete that meet the strength of light mass requirements. One of the materials most appropriate to meet these requirements is foamed concrete. The mass of foamed concrete allows for the reduction of structural dimensions which results in buildings that are lighter than conventional ones [2,3], thus reducing the risk of damage under severe earthquake conditions, especially in high rise buildings [4]. The mass of foamed concrete ranges from 1200 to 1800 kg/m³ and is included in the category of lightweight concrete. In this study, lightweight concrete was used as a material for wall panel models. The concrete consisted of Portland Composite Cement (PCC), expanded polystyrene (EPS), a foam agent, and water [5]. The use of EPS contributed to the hydrophobic qualities, as well as resistance to high thermal insulation and moisture, provided high durability and the ability to be formed in various sizes, along with recyclability [1,6,7,8]. Reinforced concrete panels with concrete compressive strengths of 38.0 up to 99.3 MPa can resist axial loads ranging from 191.3 to 1583.3 kN [9]. Although they are included in the non-structural system, reinforced concrete walls can affect the stiffness and strength of a building structure [1], especially when these contain openings for doors and windows [10]. A need remains for analyzing the behavior of lightweight wall panels under severe conditions, such

as lateral loads due to earthquakes. Wall panels consist of partial non-structural components that form wall units and are widely used for lightweight construction. Compared to conventional brick walls, the thinner dimension of these wall panels provides a lesser load for buildings [11]. To investigate the performance of wall panels under lateral loads due to wind and severe earthquakes, experiments were conducted [12] using five types of wall panels with variations of frame materials and insulating concrete form (ICF) grids [13]. The concrete compressive strength of ICF wall panels is 17.24 MPa and is included in structural components. In this study, monotonically-increasing static lateral loads with initial loads of 0.89-1.33 kN were applied to each specimen. The maximum lateral drifts ranged from 19.30 mm to 22.60 mm and 41.66 mm to 67.56 mm for framed and ICF wall panels, respectively. The maximum lateral loads ranged from 17.81 kN to 20.25 kN and 124.06 kN to 152.33 kN for framed and ICF wall panels, respectively. These experiments showed that ICF wall panels could resist higher lateral loads than the various framed wall panels that were tested [13,14]. Reinforced concrete openings in wall panels with slenderness ratios of 30, 35, and 40 were tested under uniformly distributed axial loads in one-way and two-way directions. The wall panels were reinforced by wire mesh in the center of the cross-sections. Each opening corner was reinforced diagonally to prevent shear cracks. The one-way wall panels showed typical single-curvature bending failures in horizontal cracks, while the two-way

*sitiaisyahn@ft.unsri.ac.id

wall panels showed typical double-curvature bending failures in diagonal cracks along the corners. The curves of load-deflection of the normal and high strength concrete wall panels were more non-linear and linear, respectively, than at the beginning of the loading history [9]. Six thin concrete wall panels with various aspect ratios (height/length) and concrete strengths were subjected to axial-eccentric uniformly-distributed loads in a two-way direction. The materials used in the experiments were normal and high-strength concrete, which consisted of Reactive Powder Concrete (RPC). The results of the experiments showed that an increase in aspect ratios decreased axial loads in normal concrete wall panels, while the opposite effect occurred in the RPC wall panels. The loads increased in the higher range of normal concrete strength, while the opposite effect occurred in the RPC wall panels. The deflections increased in the higher aspect ratios of the normal concrete wall panels, while the opposite effect occurred in the RPC wall panels [14]. Previous studies have used various dimensions of wall panels; these include concrete wall panels with lengths and heights of 1200 mm, 1400 mm, and 1600 mm and all having the same 40 mm thickness. Openings that served as windows and doors affected the main strength of the walls. Overall, the behavior of reinforced concrete walls with openings was effected by the geometry, supporting conditions, material properties, and dimensions, as well as the number of openings and their locations [15]. A previous study used wall panels made of lightweight concrete which were subjected to lateral loads. Some finite element models were used to predict specimen behavior; these showed close-crack patterns and load-deflection curves. Every two precast wall panels was connected with dowels, which indicated that having more dowel connections increased the resistance of the wall panels to lateral loads and reduced deformations [16]. Although non-structural lightweight concrete wall panels are widely used, their behavior under lateral loads still needs to be investigated, especially in high-risk earthquake zones. This study aims to determine the performance of lightweight concrete wall panel models that are subjected to static lateral loads until the ultimate condition, using a finite element method program by varying the dimensions, reinforcements, and openings. Efforts were made to assess the performance of these wall panel models under static lateral loads. By using an analysis of the correlation between load-deformation, stiffness, ductility, and deformation, information could be obtained about the behavior of these panel models under severe earthquake loads. In the past, researchers have conducted studies of wall panel behavior using the finite element method in numerical modelings. They reported that a prediction of the behavior of wall panel models in terms of correlation of load-deformation, stiffness, ductility, and temperature effects could be obtained by using numerical modelings [17,18]. The wall panel models were simulated as bearing elements. This information was taken into consideration when replacing the thick-

er precast non-composite walls with thin-shell concrete sandwich panels [17]. Numerical modelings have also been used to predict the effect of insulation in resisting heat in the occurrence of fires. The results showed that the temperature-time curves of the numerical modeling were similar with the experimental specimens [18]. A previous study on the effect of sandwich panels in ballistic performance and energy absorption using numerical modelings has also been made. This study analyzed the correlation between residual velocity and the shape of the projectiles that impacted the panel models. The numerical results achieved were in good agreement with the literature [19].

MATERIALS AND METHODS

The material properties for modeling input in the ANSYS program used in this study referred to previous laboratory research results [5,20]. The materials used were foamed lightweight concrete with EPS and wire mesh, which are described in the following subchapter: Materials. It was necessary to use non-linear modeling to present the behavior of the materials that formed the wall panels.

Finite Element Method

The finite element method (FEM) is a numerical method that breaks down domains into several subdomains, or finite elements with systematic estimation, to build solutions. Three points need to be taken into consideration when using this method [21]:

- Physical phenomena used to analyze the case and determine the deformation, critical areas, stress, and cracks.
- Discretization to divide domains into smaller sub-domain (finite elements). Sub-domains are regions that are bounded by lines of elements which connect between nodes.
- Assumption of linear functions for all sub-domain responses. The solution to the responses is obtained from iterations.

The ANSYS program was used for the non-linear analysis. The concrete materials, wire mesh, and steel plates were modeled using Solid65 (8-node), Link180 (2-node), and Solid45 (8-node) elements, respectively. Solid65 was used to model the behaviour of concrete materials; i.e., brittle and unsuitable in resisting tensile forces. Link180 was used for modeling wire mesh with high ductility, while an analysis of the behavior of the steel plates was performed by Solid45 [22]. The ANSYS analysis was carried out in this study by subjecting the wall panel models to lateral loads. ANSYS uses the Newton-Raphson method to solve non-linear equation problems to obtain deformations through direct iterations. This process can be described in Equations (1) and (2) [21]:

$$[K]\{u\} = \{F\} \quad (1)$$

$$\{u^{r+1}\} = [K(u^r)]^{-1}\{F\} \quad (2)$$

where $[K]$, $\{u\}$, $\{F\}$ are the stiffness matrix, the deformation vector, and the load vector, respectively; $\{u^{r+1}\}$ is an approximation of $(r+1)$ -iteration. This will be convergent for an increased r when the values of $\{u^r\}$ are close to $\{u^{r+1}\}$ with minimum deviation. The non-linear equilibrium was solved using the Newton-Raphson iteration method [23].

Materials

The materials of the wall panel used in this study consisted of lightweight foamed concrete and wire mesh. Table 1 shows the stress and strain properties of the lightweight foamed concrete using EPS. The material properties were: mass density, modulus elasticity, compressive strength, and the tensile strength of the foamed concrete, which were: 832.26 kg/m³, 4900 MPa, 5.224 MPa, and 0.2612 MPa, respectively [5].

Table 1: Stress-strain curve property of foamed concrete age 28 days [5]

No.	Stress (MPa)	Strain (mm/mm)	No.	Stress (MPa)	Strain (mm/mm)
1	0	0	10	2.659	0.00101
2	0.147	0.00003	11	2.930	0.00109
3	0.439	0.00012	12	3.241	0.00116
4	0.754	0.00025	13	3.662	0.00124
5	1.094	0.00042	14	3.831	0.00135
6	1.399	0.00058	15	4.366	0.00183
7	1.754	0.00070	16	4.672	0.00205
8	1.950	0.00081	17	4.858	0.00212
9	2.386	0.00095	18	5.224	0.00235

The wall panel models were reinforced with wire mesh that was 4 mm in diameter with a spacing of 150 mm. Figure 1 shows the stress and strain relation of the wire mesh in an ascending curve. The modulus elasticity (E_s), yield strain (ϵ_s), yield strength (f_y), and ultimate strength (f_u) were: 177,570.19 MPa, 0.002562, 424.52 MPa, and 538.68 MPa, respectively [20].

Stiffness and Deformation Ductility

Stiffness is dependent on structural configuration, dimension, member behavior, and material properties [24]. Stiffness (K) performs the load (F) to deformation (δ) ratio [25], as described in Equation (3):

$$K = \frac{F}{\delta} \quad (3)$$

Deformation ductility (μ) is the ratio of ultimate to yield conditions of the deformations (δ_u and δ_y , respectively) [26, 27], as follows in Equation (4):

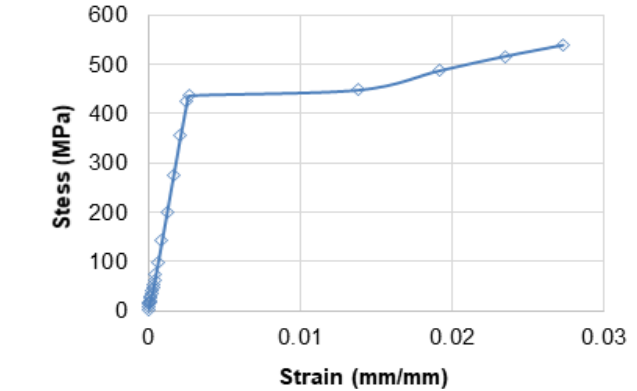


Figure 1: Curve of the stress-strain property of wire mesh 4 mm in diameter

$$\mu = \frac{\delta_u}{\delta_y} \quad (4)$$

Methodology

In this research, lightweight concrete wall panel models were subjected to incremental static lateral loads until the ultimate condition. The wall panel models varied in dimension, reinforcement (wire mesh), and openings. The analysis was conducted using ANSYS as a finite element method program. The lateral static loads were applied on steel plates on the left and top of the panels and increased by 200 N until the panels collapsed. The analysis results were depicted in curves that showed a correlation between static lateral loads and lateral deflections in representing the performance of each wall panel model.

Some assumptions were made in the modeling:

1. The wire mesh had fully bonded to the concrete.
2. Anchored wire mesh modeled as fixed-end restraints

Geometrical Data Model

As seen in Table 2, 24 wall panel models with variations in dimension, wire mesh (reinforcement), and openings were used. Letters H, L, T, W, and O represent height, length, thickness, wire mesh, and double-square openings, respectively. Table 3 shows the aspect ratio (H/L) and slenderness ratios (H/T) of each wall panel model. The loading setup of each wall panel model and the lateral load was based on the code in Figure 2 [28]. Wire mesh was anchored to the fixed base, and each panel was firmly bolted to the loading fixture. The height and width of each square opening was 200 mm. Figure 3 shows the dimension of wall panel models numbered 1 to 18 (Table 2) with various thicknesses and reinforcements. Figure 4 shows the dimensions of the concrete panel models numbered 19 to 24 (Table 2) with double-square openings without and with reinforcements. There were three diagonal steel bars in the corner of each opening; these were 4 mm in diameter, with a length of 140 mm, the wire mesh in the wall panels having a 50 mm spacing.

Table 2: Dimensions of the wall panel models

No.	Wall Panel Models	H	L	T
		(mm)	(mm)	(mm)
1	1000H.40T	1000	1500	40
2	1000H.50T	1000	1500	50
3	1000H.60T	1000	1500	60
4	1500H.40T	1500	1500	40
5	1500H.50T	1500	1500	50
6	1500H.60T	1500	1500	60
7	2000H.40T	2000	1500	40
8	2000H.50T	2000	1500	50
9	2000H.60T	2000	1500	60
10	1000H.40T.W	1000	1500	40
11	1000H.50T.W	1000	1500	50
12	1000H.60T.W	1000	1500	60
13	1500H.40T.W	1500	1500	40
14	1500H.50T.W	1500	1500	50
15	1500H.60T.W	1500	1500	60
16	2000H.40T.W	2000	1500	40
17	2000H.50T.W	2000	1500	50
18	2000H.60T.W	2000	1500	60
19	1500H.40T.O	1500	1500	40
20	1500H.50T.O	1500	1500	50
21	1500H.60T.O	1500	1500	60
22	1500H.40T.W.O	1500	1500	40
23	1500H.50T.W.O	1500	1500	50
24	1500H.60T.W.O	1500	1500	60

Table 3: The aspect and slenderness ratios

No.	Wall Panel Models	Wire Mesh	(H/L)	(H/T)
1	1000H.40T	-	0.67	25.0
2	1000H.50T	-	0.67	20.0
3	1000H.60T	-	0.67	16.7
4	1500H.40T	-	1.00	37.5
5	1500H.50T	-	1.00	30.0
6	1500H.60T	-	1.00	25.0
7	2000H.40T	-	1.33	50.0
8	2000H.50T	-	1.33	40.0
9	2000H.60T	-	1.33	33.3
10	1000H.40T.W	Ø4-150	0.67	25.0
11	1000H.50T.W	Ø4-150	0.67	20.0
12	1000H.60T.W	Ø4-150	0.67	16.7
13	1500H.40T.W	Ø4-150	1.00	37.5
14	1500H.50T.W	Ø4-150	1.00	30.0
15	1500H.60T.W	Ø4-150	1.00	25.0
16	2000H.40T.W	Ø4-150	1.33	50.0
17	2000H.50T.W	Ø4-150	1.33	40.0
18	2000H.60T.W	Ø4-150	1.33	33.3
19	1500H.40T.O	-	1.00	37.5
20	1500H.50T.O	-	1.00	30.0
21	1500H.60T.O	-	1.00	25.0
22	1500H.40T.W.O	Ø4-150	1.00	37.5
23	1500H.50T.W.O	Ø4-150	1.00	30.0
24	1500H.60T.W.O	Ø4-150	1.00	25.0

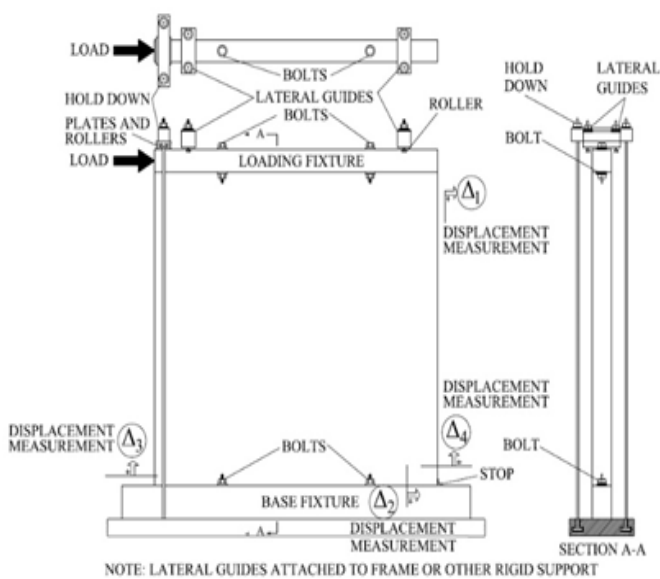


Figure 2: Set up of lateral loading on vertical panels [27]

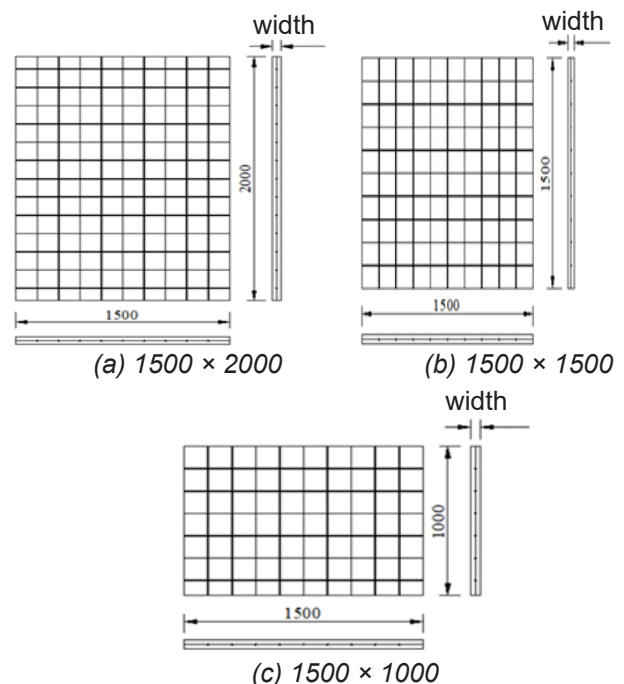


Figure 3: Dimensions of the wall panel models

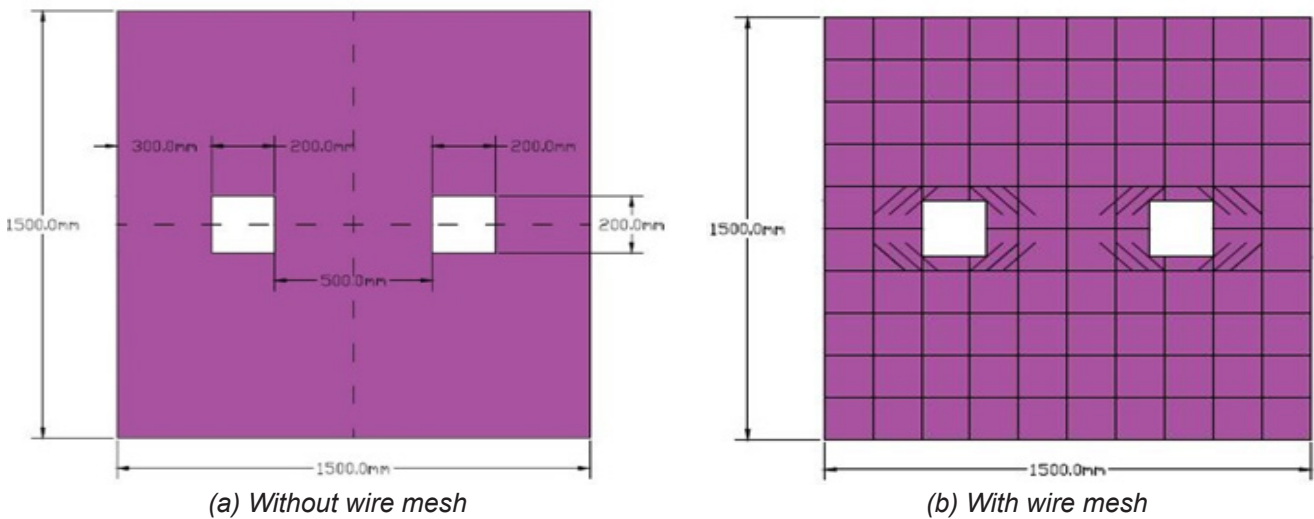


Figure 4: Dimensions of the wall panel models with openings

RESULTS AND DISCUSSION

The incremental lateral static loads pushed against the wall panel models, which resulted in lateral deformation. The lateral deformation values varied and depended on the reinforcement, aspect ratio, slenderness, and number of openings.

Correlation Between Load and Deformation

The correlation between lateral loads and deformations in the wall panel models with various heights and thicknesses without wire mesh is shown in Figures 5 to 7. The thicker wall panel models showed higher resistance performance than other models of the same height and length. Wall panel models with thicknesses of 60 mm provided greater stiffness, yield, and ultimate loads than the thinner wall panel models. The wall panel model with a height of 2000 mm and a thickness of 60 mm showed a higher lateral deformation than other models with the same thickness.

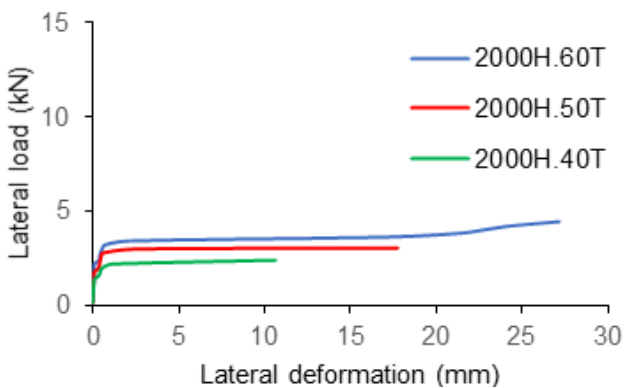


Figure 5: Curves showing lateral load-lateral deformation of wall panel models having 2000 mm height without wire mesh

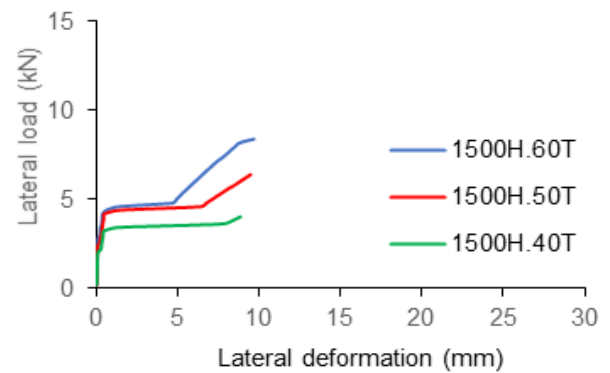


Figure 6: Curves showing the lateral load-lateral deformation of wall panel models having 1500 mm height without wire mesh

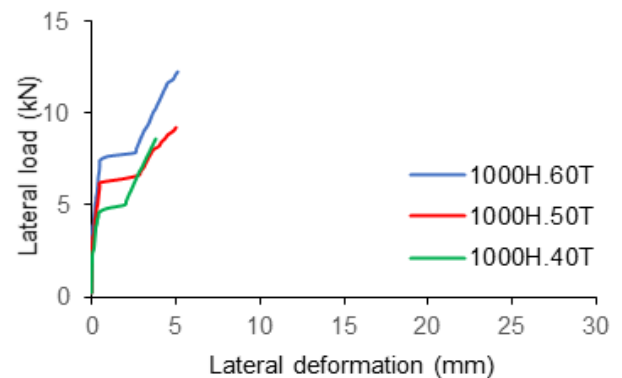


Figure 7: Curves showing lateral load-lateral deformation of wall panel models having 1000 mm height without wire mesh

Figures 8 through 10 show the correlation between lateral load-lateral deformation of wall panel models having wire mesh and height variations of 2000 mm, 1500 mm, 1000 mm and the same 1500 mm lengths. All wall panel models with wire mesh performed better against lateral loads than wall panel models of the same dimension

without wire mesh. The wall panel models with wire mesh with a thickness of 60 mm showed higher stiffness, yield and ultimate load-carrying than other wall panel models with thicknesses of 40 and 50 mm. This behavior is similar to that of previous research results [29]. Wall panel models with a height of 1000 mm achieved the highest lateral loads results due to having greater stiffness than other wall panels. The largest lateral deformations were seen in the tallest wall panels, those of 2000 mm, due to having more flexible behavior than the other panels.

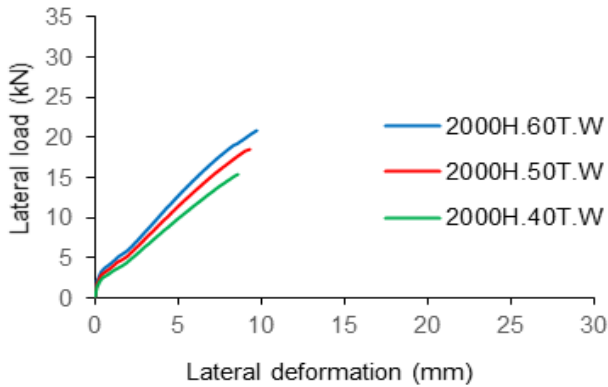


Figure 8: Curves showing lateral load-lateral deformation of wall panel models having 2000 mm height with wire mesh

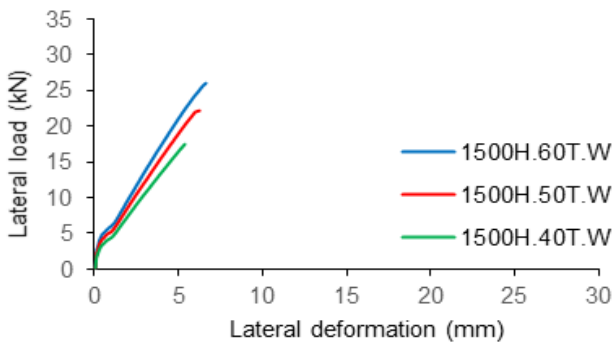


Figure 9: Curves showing lateral load-lateral deformation of wall panel models having 1500 mm height with wire mesh

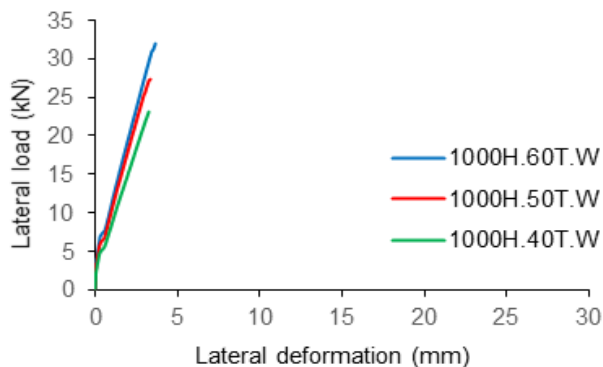


Figure 10: Curves showing lateral load-lateral deformation of wall panel models having 1000 mm height with wire mesh

The wall panel models with double-square openings performed the same as solid wall panel models, as seen in Figures 11 and 12. The thickest wall panel models, with or without wire mesh, carried higher lateral loads than other wall panel models. The use of wire mesh influenced their stiffness, ensuring that all reinforced wall panel models had less lateral deformation than the unreinforced panel models.

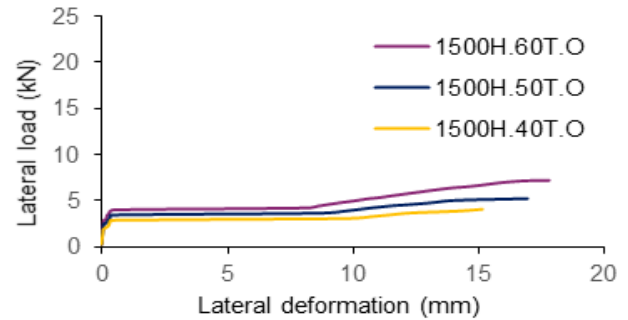


Figure 11: Curves showing lateral load-lateral deformation of wall panel models with double-square openings and having 1500 mm height and 1500 mm length without wire mesh

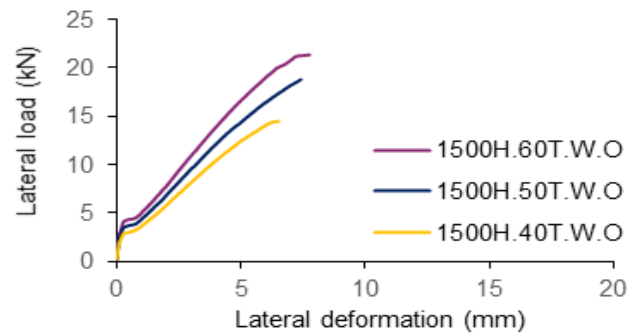


Figure 12: Curves showing lateral load-lateral deformation of wall panel models with double-square openings and having 1500 mm height and 1500 mm length with wire mesh

Openings in wall panels will result in decreased resistance performance against lateral loads [30]. Three solid-wall and three wall panel models with double-square openings without wire mesh were compared when performing lateral load resistance, as shown in Figure 13. These six wall panel models were all 1500 mm in height and 1500 mm in length. The two-wall panel model thicknesses without wire mesh were 40 mm, 50 mm, and 60 mm. All wall panel models with double-square openings achieved longer deformations with lower lateral yield and ultimate loads due to having less stiffness than the solid panel models. Similar behavior was found in solid wall panel models and wall panel models with three double-square openings with wire mesh, as seen in Figure 14. The dimensions of all the wall panel models were 1500 mm in height and 1500 mm in length. 1500 mm in height and 1500 mm in length. The thicknesses of each two-wall panel model with wire mesh were: 40

mm, 50 mm, and 60 mm. All wall panel models with double-square openings had longer deformations and lower lateral yield and ultimate loads due to having less stiffness than the solid panel models. The deformations of all solid wall panel models with double-square openings and wire mesh were less than those without wire mesh due to their higher stiffness. The rate of lateral loads achieved by all of the wall panel models with wire mesh was higher than those without wire mesh because of their higher nominal moment.

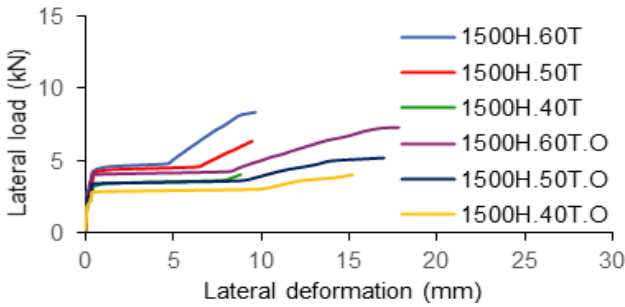


Figure 13: Curves showing lateral load-lateral deformation of wall panel models with solid and double-square openings and having 1500 mm of height and 1500 mm of length without wire mesh

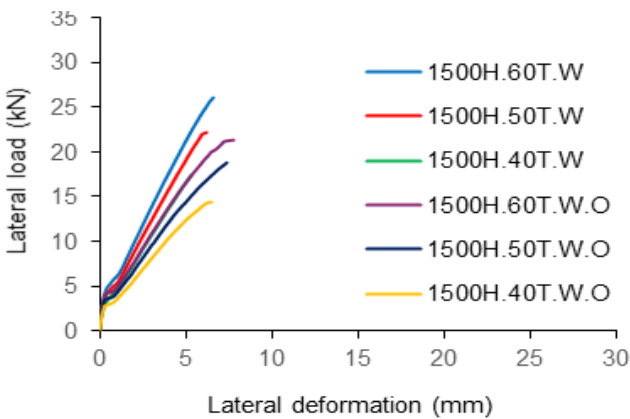


Figure 14: Curves showing lateral load-lateral deformation of wall panel models with solid and double-square openings having 1500 mm of height and 1500 mm of length with wire mesh

The loads and the deformations in yield and ultimate conditions are shown in Tables 4 and 5. All wire mesh wall panel models showed higher ultimate lateral loads than wall panels without wire mesh of the same thickness. The yield points were determined based on a code [31], while the ultimate points were in the maximum load and deformation conditions. The yield and ultimate lateral loads and the yield and ultimate lateral deformations increased as the thickness varied from 40 to 60 mm, both on unreinforced and wire mesh-enforced wall panel models. The openings reduced the stiffness of the wall panel models, thus increasing the deformation.

Table 4: Yield lateral loads and deformations

No.	Wall Panel Models	Yield Condition	
		Lateral Load	Lateral Deformation
		F_v (kN)	δ_v (mm)
1	1000H.40T	4.40	0.409
2	1000H.50T	6.00	0.477
3	1000H.60T	7.20	0.493
4	1500H.40T	3.20	0.458
5	1500H.50T	4.20	0.480
6	1500H.60T	4.40	0.585
7	2000H.40T	2.00	0.577
8	2000H.50T	2.80	0.617
9	2000H.60T	3.20	0.742
10	1000H.40T.W	4.80	0.291
11	1000H.50T.W	6.20	0.323
12	1000H.60T.W	7.20	0.357
13	1500H.40T.W	3.20	0.343
14	1500H.50T.W	4.20	0.410
15	1500H.60T.W	5.00	0.472
16	2000H.40T.W	2.40	0.404
17	2000H.50T.W	3.00	0.447
18	2000H.60T.W	3.60	0.513
19	1500H.40T.O	2.40	0.309
20	1500H.50T.O	3.40	0.376
21	1500H.60T.O	4.00	0.496
22	1500H.40T.W.O	2.60	0.227
23	1500H.50T.W.O	3.40	0.262
24	1500H.60T.W.O	4.20	0.369

The thickness, height, and openings influenced the lateral loads and deformations in yield and ultimate conditions. The thicker wall panels had greater resistance to deformation. The more ductile behavior of wall panel models with wire mesh made it possible to achieve longer deformation. Tables 6 and 7 show the percentages of load and deformation of each panel model compared to the panel models that had 60 mm thicknesses; these groups are divided according to height in yield and ultimate conditions, respectively.

Table 5: Ultimate lateral loads and deformations

No.	Wall Panel Models	Yield Condition	
		Lateral Load	Lateral Deformation
		F_u	δ_u
		(kN)	(mm)
1	1000H.40T	8.40	3.644
2	1000H.50T	9.20	4.941
3	1000H.60T	12.20	5.134
4	1500H.40T	4.00	8.870
5	1500H.50T	6.40	9.522
6	1500H.60T	8.40	9.676
7	2000H.40T	2.40	10.586
8	2000H.50T	3.06	17.763
9	2000H.60T	4.40	27.151
10	1000H.40T.W	23.00	3.232
11	1000H.50T.W	27.40	3.288
12	1000H.60T.W	32.00	3.611
13	1500H.40T.W	17.40	5.365
14	1500H.50T.W	22.20	6.218
15	1500H.60T.W	26.00	6.591
16	2000H.40T.W	15.40	8.587
17	2000H.50T.W	18.40	9.285
18	2000H.60T.W	20.80	9.704
19	1500H.40T.O	4.00	15.170
20	1500H.50T.O	5.20	16.938
21	1500H.60T.O	7.25	17.804
22	1500H.40T.W.O	14.45	6.534
23	1500H.50T.W.O	18.80	7.413
24	1500H.60T.W.O	21.35	7.787

Table 6: Percentages of yield load and deformation

No.	Wall Panel Models	Yield Condition	
		Lateral Load	Lateral Deformation
		(%)	(%)
1	1000H.40T	61.11	82.98
2	1000H.50T	83.33	96.75
3	1000H.60T	100.00	100.00
4	1500H.40T	72.73	78.29
5	1500H.50T	95.45	81.97
6	1500H.60T	100.00	100.00
7	2000H.40T	62.50	77.78
8	2000H.50T	87.50	83.08
9	2000H.60T	100.00	100.00
10	1000H.40T.W	66.67	81.46
11	1000H.50T.W	86.11	90.60
12	1000H.60T.W	100.00	100.00
13	1500H.40T.W	64.00	72.73
14	1500H.50T.W	84.00	86.90
15	1500H.60T.W	100.00	100.00
16	2000H.40T.W	66.67	78.62
17	2000H.50T.W	83.33	87.00
18	2000H.60T.W	100.00	100.00
19	1500H.40T.O	60.00	62.29
20	1500H.50T.O	85.00	75.70
21	1500H.60T.O	100.00	100.00
22	1500H.40T.W.O	61.90	61.47
23	1500H.50T.W.O	80.95	70.97
24	1500H.60T.W.O	100.00	100.00

Stiffness and Deformation Ductility

Tables 8 and 9 show the stiffness and deformation ductility of each panel model, respectively. The yield and ultimate stiffnesses were influenced by the thickness and wire mesh reinforcement in the wall panel models. The thicker wall panel models achieved higher levels of stiffnesses. Stiffnesses were also higher in wall panel models with wire mesh as opposed to panels without wire mesh but with the same thicknesses. Lower ductility values were also achieved by the panel models with wire mesh. Table 8 also shows that the wall panel model with a height of 1000 mm, length of 1500 mm, and thickness of 60 mm with wire mesh (number 12) had the highest stiffness, which means this model also performed the best strength in resisting lateral loads. Based on all of the solid wall panel models (Nos. 1-18), those with a height of 2000 mm and a thickness of 60 mm (Table 9, number 9) without wire mesh had the highest deformation ductility;

that of 36.59. Thus, it can be seen that the tallest and thickest panels had the best ductility. This behavior was also observed in previous research [32].

The inclusion of wire mesh significantly reduced deformation ductility in the wall panel models (Nos. 10 to 18) compared to models of the same dimension without wire mesh [26]. However, models with openings showed the opposite behavior (Nos. 19-24). The best ductility among wall panels with openings was achieved by the thinnest panel models without wire mesh (1500H.40T.O). This also reveals that openings influence the behavior of wall panel models under lateral loads when compared to solid panel models without openings. Table 9 shows that in all the solid models without wire mesh (numbers 1-9), the tallest model, with height of 2000 mm, length of 1500 mm, and thickness of 60 mm (number 9), achieved the best ductility due to having the largest ultimate deformation. In all solid models with wire mesh (numbers 10-18),

Table 7: Percentages of ultimate load and deformation

No.	Wall Panel Models	Yield Condition	
		Lateral Load	Lateral Deformation
		(%)	(%)
1	1000H.40T	68.85	70.97
2	1000H.50T	75.41	96.24
3	1000H.60T	100.00	100.00
4	1500H.40T	47.62	91.67
5	1500H.50T	76.19	98.41
6	1500H.60T	100.00	100.00
7	2000H.40T	54.55	38.99
8	2000H.50T	69.55	65.42
9	2000H.60T	100.00	100.00
10	1000H.40T.W	71.88	89.51
11	1000H.50T.W	85.63	91.05
12	1000H.60T.W	100.00	100.00
13	1500H.40T.W	66.92	81.40
14	1500H.50T.W	85.38	94.35
15	1500H.60T.W	100.00	100.00
16	2000H.40T.W	74.04	88.49
17	2000H.50T.W	88.46	95.68
18	2000H.60T.W	100.00	100.00
19	1500H.40T.O	55.17	85.21
20	1500H.50T.O	71.72	95.14
21	1500H.60T.O	100.00	100.00
22	1500H.40T.W.O	67.68	83.91
23	1500H.50T.W.O	88.06	95.19
24	1500H.60T.W.O	100.00	100.00

Table 8: Yield and ultimate stiffnesses

No.	Wall Panel Models	Lateral Load	Lateral Deformation
		K_v	K_u
		(kN)	(mm)
1	1000H.40T	10.75	2.31
2	1000H.50T	12.57	1.86
3	1000H.60T	14.59	2.38
4	1500H.40T	6.99	0.45
5	1500H.50T	8.76	0.67
6	1500H.60T	7.52	0.87
7	2000H.40T	3.47	0.23
8	2000H.50T	4.54	0.17
9	2000H.60T	4.31	0.16
10	1000H.40T.W	16.51	7.12
11	1000H.50T.W	19.18	8.33
12	1000H.60T.W	20.17	8.86
13	1500H.40T.W	9.32	3.24
14	1500H.50T.W	10.24	3.57
15	1500H.60T.W	10.60	3.94
16	2000H.40T.W	5.94	1.79
17	2000H.50T.W	6.72	1.98
18	2000H.60T.W	7.01	2.14
19	1500H.40T.O	7.76	0.26
20	1500H.50T.O	9.05	0.31
21	1500H.60T.O	8.06	0.41
22	1500H.40T.W.O	11.46	2.21
23	1500H.50T.W.O	12.98	2.54
24	1500H.60T.W.O	11.38	2.74

the model with a height of 2000 mm, length of 1500 mm, and thickness of 40 mm (number 16) achieved the best ductility. In all models with openings and without wire mesh (numbers 19-21) and with wire mesh (numbers 22-24), the models with heights of 1500, lengths of 1500 mm, and thicknesses of 40 mm achieved the best ductility. These results show that thickness and reinforcement with wire mesh influence ductility.

Deformation

The highest deformation ranges among all the solid wall panel models are at the top, as depicted in red. The red area depicts lightweight concrete and steel plate materials. Steel plates prevented wall panels from deforming out of the plane [12]. Wall panel models without wire mesh showed much greater deformations than wall panel models with wire mesh. These greater deformations were located around halfway the height of the panel on the lefthand side. The distribution and magnitude focused

deformations appeared on the lefthand sides of the wall panels without wire mesh, which are represented in dark blue (Figure 15). All panel models, with or without wire mesh, showed that the taller wall panel models had a greater number of maximum lateral deformations. This is because the points observed were at the top of the wall panel models. Models with the same dimensions showed that wire mesh significantly reduced lateral deformation due to having greater stiffness (Figure 16). Comparing wall panel models of the same height and length showed that the dimension of thickness resulted in fewer maximum deformations.

Table 9: Stiffness ratio and ductility

No.	Wall Panel Models	Stiffness Ratio	Ductility
		K_u/K_v	$\mu = \delta_u/\delta_v$
1	1000H.40T	0.21	8.90
2	1000H.50T	0.15	10.35
3	1000H.60T	0.16	10.41
4	1500H.40T	0.06	19.37
5	1500H.50T	0.08	19.86
6	1500H.60T	0.12	16.54
7	2000H.40T	0.07	18.34
8	2000H.50T	0.04	28.81
9	2000H.60T	0.04	36.59
10	1000H.40T.W	0.43	11.12
11	1000H.50T.W	0.43	10.17
12	1000H.60T.W	0.44	10.12
13	1500H.40T.W	0.35	15.63
14	1500H.50T.W	0.35	15.16
15	1500H.60T.W	0.37	13.97
16	2000H.40T.W	0.30	21.27
17	2000H.50T.W	0.30	20.78
18	2000H.60T.W	0.31	18.90
19	1500H.40T.O	0.03	49.06
20	1500H.50T.O	0.03	45.07
21	1500H.60T.O	0.05	35.87
22	1500H.40T.W.O	0.19	28.79
23	1500H.50T.W.O	0.20	28.29
24	1500H.60T.W.O	0.24	21.09

Wall panel models with openings and without wire mesh had negative deformations halfway the height on the lefthand side. This indicates bending in the tensile areas which changed the shape of the wall panel models. The middle and righthand sides were more dominated by positive deformations due to compressive conditions. The wall panels reinforced with wire mesh showed an evenly distributed spread of negative deformations in the panels nearest the fixed supports. In contrast, positive deformations were dominant in the middle and upper parts of the panels (Figure 17). All of the wall panel models without wire mesh achieved greater minimum and maximum deformations due to having less stiffness. The thinner panels had larger deformations around the openings, while the thicker panels showed increased deformations. The minimum and maximum deformations of the wall panels are shown in Table 10.

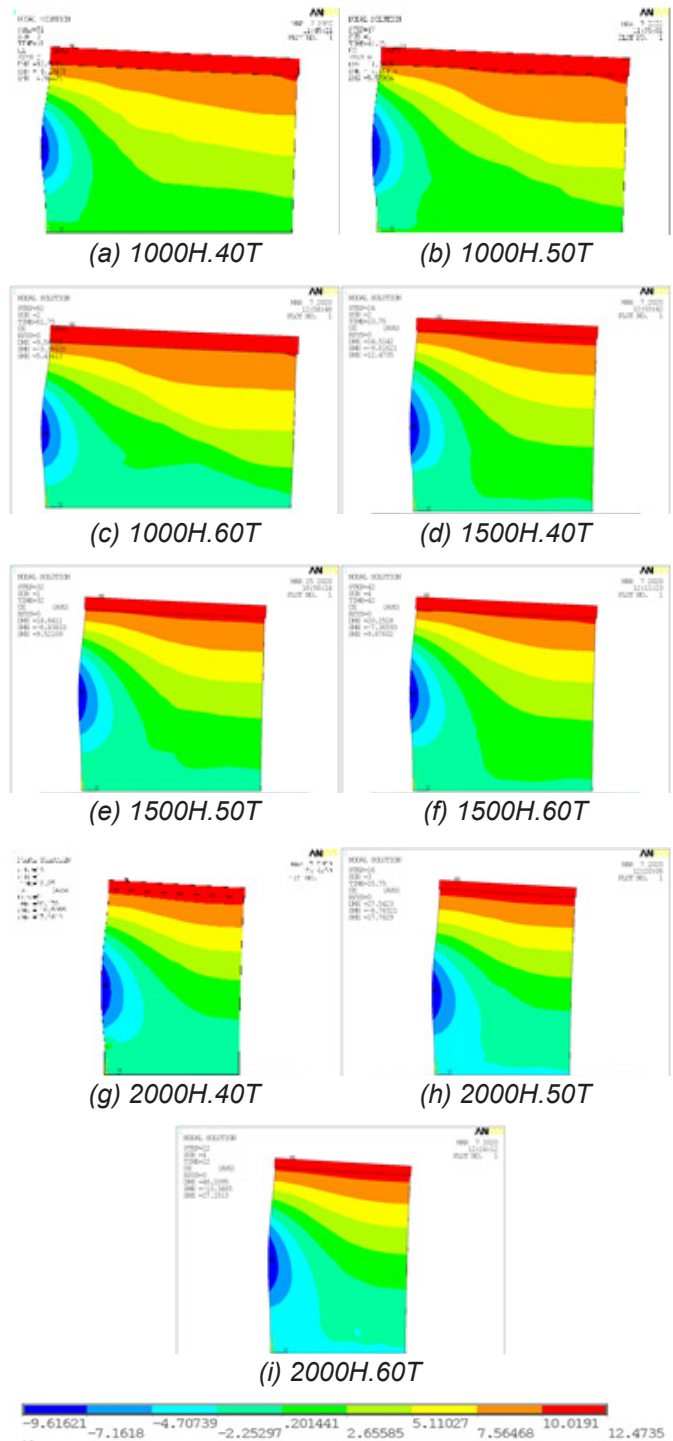


Figure 15: Maximum lateral deformations of solid wall panel models without wire mesh with different spreading of deformation

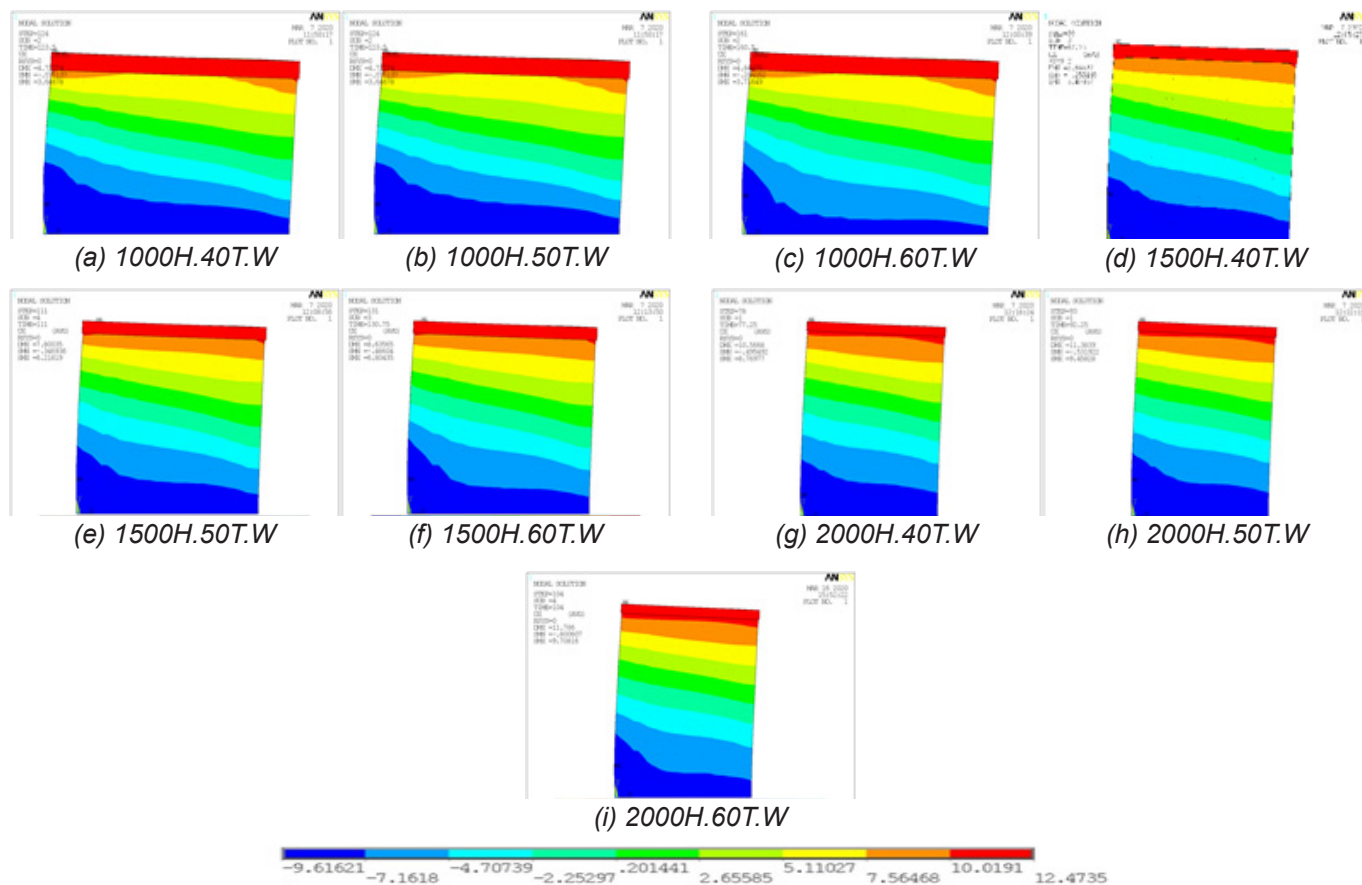


Figure 16: Maximum lateral deformations of solid wall panels with wire mesh with different spreading of deformation

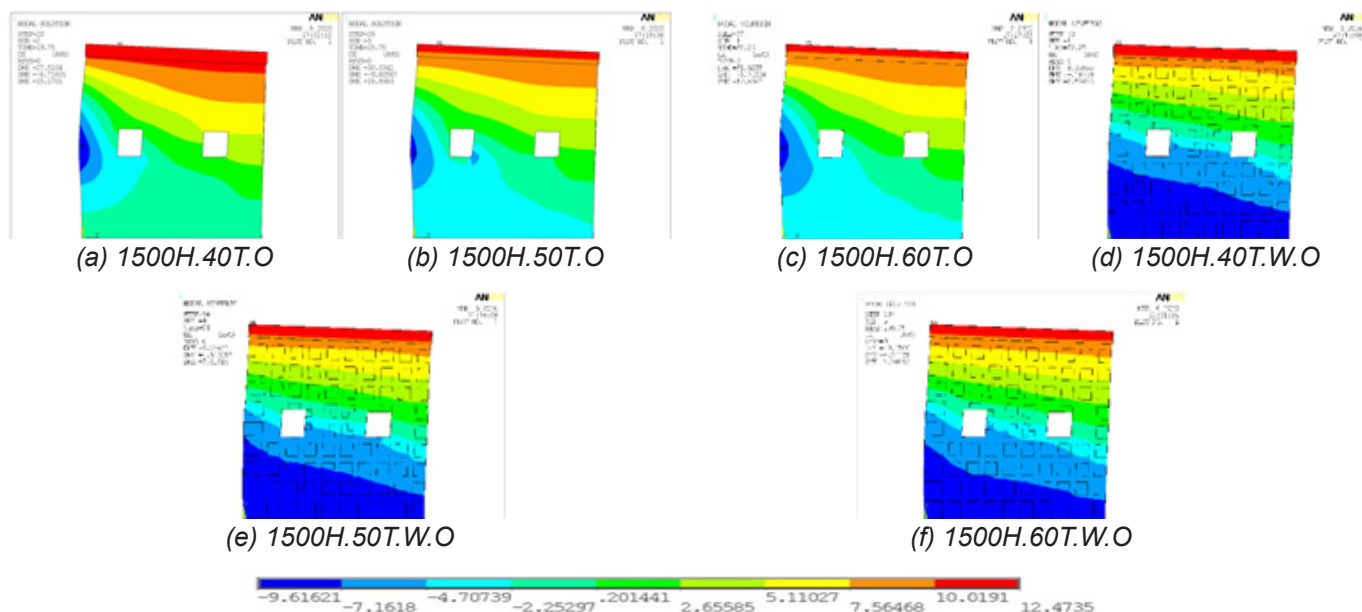


Figure 17: The lateral deformation of wall panels with wire mesh and with or without openings with different spreading of deformation

Wall panel models with openings and without wire mesh had negative deformations halfway the height on the lefthand side. This indicates bending in the tensile areas which changed the shape of the wall panel models. The middle and righthand sides were more dominated by positive deformations due to compressive conditions. The wall panels reinforced with wire mesh showed an evenly distributed spread of negative deformations in the panels nearest the fixed supports. In contrast, positive deformations were dominant in the middle and upper parts of the panels (Figure 17). All of the wall panel models without wire mesh achieved greater minimum and maximum deformations due to having less stiffness. The thinner panels had larger deformations around the openings, while the thicker panels showed increased deformations. The minimum and maximum deformations of the wall panels are shown in Table 10.

Table 10: Lateral deformation of wall panels

No.	Wall Panel Models	Minimum Deformation	Maximum Deformation
		δ_{\min} (mm)	δ_{\max} (mm)
1	1000H.40T	-4.191	4.984
2	1000H.50T	-4.481	5.539
3	1000H.60T	-3.394	5.434
4	1500H.40T	-9.616	12.474
5	1500H.50T	-9.481	13.169
6	1500H.60T	-7.366	9.676
7	2000H.40T	-10.596	17.942
8	2000H.50T	-8.783	17.763
9	2000H.60T	-13.347	27.151
10	1000H.40T.W	-0.075	3.647
11	1000H.50T.W	-0.179	3.872
12	1000H.60T.W	-0.293	3.716
13	1500H.40T.W	-0.253	5.480
14	1500H.50T.W	-0.347	6.218
15	1500H.60T.W	-0.486	6.804
16	2000H.40T.W	-0.495	8.770
17	2000H.50T.W	-0.532	9.458
18	2000H.60T.W	-0.801	9.708
19	1500H.40T.O	-8.197	15.170
20	1500H.50T.O	-9.807	16.940
21	1500H.60T.O	-10.197	17.800
22	1500H.40T.W.O	-0.187	6.530
23	1500H.50T.W.O	-0.310	7.420
24	1500H.60T.W.O	-0.512	7.790

CONCLUSIONS

This study investigated the behavior of non-structural lightweight concrete wall panel models made of EPS foamed concrete and reinforced with wire mesh. A finite element method-based program was used to obtain a non-linear analysis of 24 wall panel models subjected to lateral static loads. The results showed that the dimensions, reinforcement, and openings influence how wall panels behave in the scope of deformation, strength, stiffness, and ductility. Optimum ultimate strength and stiffness were achieved by a solid wall panel with wire mesh, having a length of 1500 mm, a height of 1000 mm, and 60 mm thickness. Evidence for this is shown in both Tables 5 and 8. The wall panel models with openings, without wire mesh, and with a height, length, and thickness of 1500 mm, 1500 mm, and 40 mm, respectively, achieved the highest ductility. Evidence for this is shown in Table 9. As this study was based on the finite element method, further validation using experimental work is still needed.

ACKNOWLEDGMENT

The authors would like to thank Universitas Sriwijaya for their funding under contract number 0179.014/UN9/SB3.LPPM.PT/2020.

REFERENCES

- Houa, H., Jia, K., Wanga, W., Qua, B., Fang, M., Qiu, C. (2019). Flexural behavior of precast insulated sandwich wall panels: Full-scale tests and design implications. *Engineering Structures*, vol. 180, pp. 750–761. <https://doi.org/10.1016/j.engstruct.2018.11.068>.
- Castillo, E. R., Almesfer, N., Saggi, O., Ingham, J. M. (2020). Lightweight concrete with artificial aggregate manufactured from plastic waste. *Construction and Building Materials*, vol. 265, 120199. <https://doi.org/10.1016/j.conbuildmat.2020.120199>.
- Niknamfar, A. H. and Eesapoor, S. (2017). Generating a Structural Lightweight Concrete. *Proc. 3rd International Conference of Science and Engineering in the Technology Era, Copenhagen*, pp. 1-18.
- Vandanapu, S. N. and Krishnamurthy, M. (2018). Seismic Performance of Lightweight Concrete Structures. *Advances in Civil Engineering*, 2105784. <https://doi.org/10.1155/2018/2105784>.
- Law, T. E. (2020). Physical and Mechanical Properties of Lightweight Concrete with Variation of EPS Diameter. The thesis of Undergraduate Program, Universitas Sriwijaya, Indralaya. (text in Indonesian)
- Khatib, J. M., Herki, B. A., and Elkordi, A. (2019). Characteristics of Concrete Containing EPS, Use of Recycled Plastics in Eco-efficient Concrete. *Civil and Structural Engineering book chapter*, pp. 137-165. <https://doi.org/10.1016/B978-0-08-102676-2.00007-4>.

7. Dixit, A., Pang, S. D., Kang, S. H., and Moon, J. (2019). Lightweight structural cement composites with expanded polystyrene (EPS) for enhanced thermal insulation. *Cement and Concrete Composites*, vol. 102, pp. 185-197. <https://doi.org/10.1016/j.cem-concomp.2019.04.023>.
8. Assaad, J. J. and Mir, A. E. (2020). Durability of polymer-modified lightweight flowable concrete made using expanded polystyrene. *Construction and Building Materials*, vol. 249, 118764. <https://doi.org/10.1016/j.conbuildmat.2020.118764>.
9. Fragomeni, S., Doh, J. H., and Lee, D. J. (2012). Behavior of Axially Loaded Concrete Wall Panels with Openings: An Experimental Study. *Advances in Structural Engineering*, vol. 15, no. 8, pp. 1345-1358. <https://doi.org/10.1260/1369-4332.15.8.1345>.
10. Tena-Colunga, A. and Liga-Paredes, A. E. (2020). Approximation of lateral stiffness for walls with two bands of openings considering slab stiffness effects. *Journal of Building Engineering*, 30, 101310. <https://doi.org/10.1016/j.jobe.2020.101310>.
11. Saltykov, I. and Bovsunovskaya, M. (2019). The comparison between the walls properties from brick and reinforced concrete of Russian orthodox temple buildings. *Proceeding of E3S Web of Conferences*, vol 110, 01065. <https://doi.org/10.1051/e3s-conf/201911001065>.
12. American Society for Testing and Materials. (2018). ASTM E 564-06 Standard Practice for Static Load Test for Shear Resistance of Framed Walls for Buildings, West Conshohocken, <https://www.astm.org/Standards/E564.htm>.
13. Mehrabi, A. (2000). In-Plane Lateral Load Resistance of Wall Panels in Residential Buildings. Prepared for the Portland Cement Association by Construction Technology Laboratories, Inc., Skokie, IL, no. 2403.
14. Mohasein, S. K., Al-Jaberi, L. A., and Ismael, A. H. (2017). Experimental Study on Structural Behavior of Thin Wall Concrete Panels Subjected to Axial Eccentric Uniformly Distributed Loading. *Journal of Engineering and Sustainable Development*, vol. 21, no. 1, pp. 51-64, http://www.jeasd.org/images/2017edition/issue_1/5.pdf.
15. Lee, D. (2003). Experimental and Theoretical Studies of Normal and High Strength Concrete Wall Panels". Doctoral Thesis, Griffith University, Queensland. <https://doi.org/10.25904/1912/695>.
16. Dunn, T. P. A. (2017). Precast Lightweight Foamed Concrete Walling, a Structural System for Low-Rise Residential Buildings. Thesis, Stellenbosch University, Stellenbosch.
17. Alchaar, A. and Abed, F. (2020). Finite element analysis of a thin-shell concrete sandwich panel under eccentric loading. *Journal of Building Engineering*, vol. 32, 101804, pp. 1-8, <https://doi.org/10.1016/j.jobe.2020.101804>.
18. Upasiri, I. R., Konthesigha, A. M. C., Nanayakkara, S. M. A., Poologanathan, K., Gatheeshgar, P., and Nuwanthika, D. (2021). Finite element analysis of lightweight composite sandwich panels exposed to fire. *Journal of Building Engineering*, vol. 32, 102329, pp. 1-15, <https://doi.org/10.1016/j.jobe.2021.102329>.
19. Khaire, N., Bhure, V., and Tiwari, G. (2020). Finite element analysis of impact response of foams in sandwich panels. *Materials Today: Proceedings*, vol. 28, pp. 2585–2590, <https://doi.org/10.1016/j.matpr.2020.05.703>.
20. Nurjannah, S. A., Budiono, B., Imran, I., and Sugiri, S. (2016). The Hysteretic Behavior of Partially Pre-Stressed Beam-Column Joint Sub-assemblages Made of Reactive Powder Concrete. *Journal of Engineering and Technological Sciences*, vol. 48 no. 5, pp. 550-570, <https://doi.org/10.5614/j.eng.technol.sci.2016.48.5.4>.
21. ANSYS, Inc. (2013). ANSYS Mechanical APDL Structural Analysis Guide, Canonsburg: SAS IP, Inc.
22. Thompson, M. K., and Thompson, J. M. (2017). ANSYS Mechanical APDL for Finite Element Analysis, Cambridge: Elsevier Inc.
23. Budiono, B., Nurjannah, S. A., and Imran, I., (2019). Non-linear Numerical Modeling of Partially Pre-stressed Beam-column Sub-assemblages Made of Reactive Powder Concrete. *Journal of Engineering and Technological Sciences*, vol. 51 no. 1, pp. 28-47, <https://dx.doi.org/10.5614/j.eng.technol.sci.2019.51.1.3>.
24. Anwar, N. and Najam, F. A. (2017). Structural Cross-Sections: Analysis and Design, Cambridge: Elsevier Science.
25. Tang, T. O. and Su, R. K. L. (2014). Shear and Flexural Stiffnesses of Reinforced Concrete Shear Walls Subjected to Cyclic Loading. *The Open Construction and Building Technology Journal*, vol. 8, pp. 104-121, <https://doi.org/10.2174/1874836801408010104>.
26. Deng, M., Zhang, W., and Yang, S. (2020). "In-plane seismic behavior of autoclaved aerated concrete block masonry walls retrofitted with high ductile fiber-reinforced concrete," *Engineering Structures*, vol. 219, 110854, <https://doi.org/10.1016/j.eng-struct.2020.110854>.
27. Sulistyorini, D. and Yasin, I. (2018). Ductility of polystyrene waste panel. *IOP Conf. Series: Materials Science and Engineering*, vol. 316, 012040, pp. 1-7. <https://doi.org/doi:10.1088/1757-899X/316/1/012040>.

28. American Society for Testing and Materials. (2015). ASTM E72-15 Standard Test Methods of Conducting Strength Tests of Panels for Building Construction, West Conshohocken, <https://www.astm.org/Standards/E72>.
29. Amran, Y. H. M., Alyousef, R., Alabduljabbar, H., Alshoudi, F., and R. S. M. Rashid. (2019). Influence of slenderness ratio on the structural performance of lightweight foam concrete composite panel. *Case Studies in Construction Materials*, vol. 10, e00226.
30. Ho, N. M., Doh, J. H., Fragomeni, S., Yang, J., Yan, K., and Guerrieri, M. (2020). Prediction of axial load capacity of concrete walls with openings restrained on three sides", *Structures*, vol. 27, pp. 1860-1875. <https://doi.org/10.1016/j.istruc.2020.08.011>.
31. American Society of Civil Engineers. (2000). Federal Emergency Management Agency (FEMA) 356 Pre-standard and Commentary for The Seismic Rehabilitation of Buildings, Virginia, pp. 3-19 to 3-20.
32. Carrillo, J. González, G., and Rubiano, A. (2014). Displacement ductility for seismic design of RC walls for low-rise housing. *Latin American Journal of Solids and Structures*, vol. 11(4), pp. 725-737.

Paper submitted: 23.02.2021.

Paper accepted: 13.07.2021.

*This is an open access article distributed under the
CC BY 4.0 terms and conditions.*